Research Square

Preprints are preliminary reports that have not undergone peer review.
They should not be considered conclusive, used to inform clinical practice,
or referenced by the media as validated information.

Organ-Specific CT Radiomics Signatures of Hepatic, Pancreatic, and Renal Parenchyma for Stratification of Glycaemic Status

Sherin Percy V

sherinpercy26@gmail.com

SRM Institute of Science and Technology

Dr. Sundarapandian subramanian

SRM Institute of Science and Technology

Dr. Senthilkumar Aiyappan

SRM Institute of Science and Technology

Research Article

Keywords: Radiomics, Tomography, X-Ray Computed, Diabetes Mellitus, Prediabetic State, Blood Glucose, Glycated Haemoglobin A

Posted Date: March 13th, 2026

DOI: https://doi.org/10.21203/rs.3.rs-8867164/v1

License: This work is licensed under a Creative Commons Attribution 4.0 International License.
Read Full License

Additional Declarations: No competing interests reported.

Organ-Specific CT Radiomics Signatures of Hepatic, Pancreatic, and Renal Parenchyma for Stratification of Glycaemic Status

[1]Sherin Percy V [1*]Dr. Sundarapandian Subramanian [2*]Dr. Senthilkumar Aiyappan

…

[1]Sherin Percy V, Department of Radiodiagnosis, SRM Medical college hospital and research Centre, SRM Institute of Science and Technology, SRM Nagar, Kattankulathur-603203, Kancheepuram, Chennai, Tamil Nadu, India.

Email address: sherinpercy26@gmail.com

[1*]Dr. Sundarapandian Subramanian, Department of Anatomy, SRM Medical college hospital and research Centre, Faculty of Medicine and Health Sciences, SRM Institute of Science and Technology, SRM Nagar, Kattankulathur-603203, Kancheepuram, Chennai, Tamil Nadu, India.

Email address: sssspandian@gmail.com **.**

[2*]Dr. SenthilKumar Aiyappan, Department of Radiodiagnosis, SRM Medical college hospital and research Centre, Faculty of Medicine and Health Sciences, SRM Institute of Science and Technology, SRM Nagar, Kattankulathur -603203, Kancheepuram, Chennai, Tamil Nadu, India.

Email address: senthila1@srmist.edu.in .

Abstract

Purpose: To evaluate organ-specific computed tomography (CT) radiomics signatures of the liver, pancreas, and kidneys for stratification of glycaemic status and to determine differential radiomic behaviour across abdominal parenchymal organs.

Methods: In this prospective study, adult patients undergoing non-contrast abdominal CT were categorised into normoglycemia, prediabetes, and diabetes groups based on fasting plasma glucose and HbA1c. Regions of interest were manually segmented in hepatic, pancreatic, and renal parenchyma. First-order attenuation features and texture features derived from GLCM, GLRLM, and GLSZM matrices were extracted using IBSI-compliant software. Organ-wise radiomic signatures were analysed for group differences and correlation with glycaemic markers. Receiver operating characteristic (ROC) analysis evaluated organ-specific stratification performance.

Results: A total of 120 patients (mean age 52 ± 11 years) were included. Hepatic mean attenuation showed significant inverse correlation with fasting glucose ($r = –0.41$, $p < 0.001$). Pancreatic entropy and renal gray-level non-uniformity demonstrated significant positive correlations with HbA1c ($r = 0.36$ and 0.32, respectively; $p < 0.01$). Organ-wise AUCs for discrimination of diabetes were: liver 0.81, pancreas 0.76, and kidney 0.72. Multi-organ fusion improved AUC to 0.87.

Conclusion: CT radiomics reveals distinct organ-specific signatures associated with glycaemic status. The liver demonstrates the strongest attenuation-based association, while the pancreas and the kidney exhibit texture-driven heterogeneity changes. Multi-organ phenotyping enhances metabolic stratification beyond single-organ assessment.

Keywords: Radiomics, Tomography, X-Ray Computed, Diabetes Mellitus, Prediabetic State, Blood Glucose, Glycated Haemoglobin A

Introduction Disorders of glucose metabolism, encompassing insulin resistance, prediabetes, and type 2 diabetes mellitus, constitute a growing global health burden with major implications for cardiovascular disease, chronic kidney disease, and non-alcoholic fatty liver disease. While biochemical markers such as fasting plasma glucose and glycated haemoglobin (HbA1c) provide systemic indices of metabolic status, they do not capture organ-level structural and microstructural alterations that accompany metabolic dysregulation. Computed tomography (CT) is widely performed in routine clinical practice and provides reproducible quantitative information regarding tissue attenuation. Reduced hepatic attenuation on non-contrast CT is an established surrogate for hepatic steatosis [32,33]. Pancreatic fat quantification and renal cortical attenuation changes have similarly been linked to metabolic dysfunction and insulin resistance [7,15]. Radiomics enables high-throughput extraction of quantitative features describing voxel intensity distributions and spatial relationships [1,2]. Radiomics methodology has matured substantially following foundational work by Lambin et al. and Aerts et al. [1,2], and subsequent standardisation through the Image Biomarker Standardisation Initiative [4]. Radiomics has demonstrated reproducibility potential when standardised feature definitions and discretisation schemes are applied [34,38]. Radiomics has been extensively investigated in oncology [3] and increasingly applied to diffuse parenchymal diseases, including hepatic steatosis and fibrosis [19,29], pancreatic pathology [9,11], and renal parenchymal abnormalities [13,16]. Despite this growing literature, most metabolic radiomics studies evaluate a single organ in isolation. Given that glucose metabolism involves coordinated dysfunction across multiple abdominal organs, a multi-organ phenotyping approach may provide a more accurate and biologically meaningful assessment of metabolic status. The present study, therefore, investigates organ-specific CT radiomics signatures of the liver, pancreas, and kidneys for the stratification of glycaemic status.

Materials and Methods This prospective cohort study included 120 adult patients undergoing clinically indicated non-contrast abdominal computed tomography (CT), who were stratified into normoglycemia (n = 40), prediabetes (n = 40), and diabetes (n = 40) groups based on fasting plasma glucose and glycated haemoglobin (HbA1c) levels in accordance with established diagnostic thresholds. All CT examinations were performed using multidetector CT scanners at 120 kVp with a slice thickness of 2.5 mm and a standard soft-tissue reconstruction kernel, without intravenous contrast administration. Manual segmentation was performed by an abdominal radiologist with five years' experience on three contiguous axial slices at standardised anatomical locations, including the right hepatic lobe (avoiding major

vessels), pancreatic body, and renal cortex of the right kidney. Radiomics features were extracted using Image Biomarker Standardisation Initiative (IBSI)-compliant software [4]. Extracted feature classes comprised first-order statistics (mean, standard deviation, skewness, kurtosis), Gray-level co-occurrence matrix (GLCM), Gray-level run-length matrix (GLRLM), and Gray-level size zone matrix (GLSZM) features, consistent with established radiomics frameworks and prior methodological literature [1,14]. Before feature calculation, voxel intensities were discretised using a fixed bin width approach, as the discretisation strategy has been shown to significantly influence radiomics feature stability and reproducibility [35,36]. Feature robustness was evaluated by assessing reproducibility using the intraclass correlation coefficient (ICC) in a randomly selected subset of cases undergoing repeat segmentation, in accordance with previously reported radiomics reproducibility methodologies [34,37]. Features demonstrating poor reproducibility (ICC < 0.75) were excluded from further analysis, consistent with recommendations in texture analysis and radiomics quality assessment literature [22,40], thereby ensuring retention of stable and reliable imaging biomarkers for downstream statistical and modelling analyses. Statistical analyses included one-way analysis of variance (ANOVA) for group-wise comparisons, Pearson correlation for assessment of associations with metabolic biomarkers, receiver operating characteristic (ROC) analysis for evaluation of discriminatory performance, and construction of an exploratory random forest model for multi-organ feature integration. All statistical tests were two-sided, and a p-value < 0.05 was considered statistically significant.

Results

Study Population Characteristics: A total of 120 participants were included, comprising 40 individuals with normoglycemia, 40 with prediabetes, and 40 with diabetes. Baseline demographic and metabolic characteristics are summarised (Table 1). Mean age and body mass index (BMI) increased progressively across glycaemic strata ($p = 0.01$ and $p < 0.001$, respectively). Fasting plasma glucose and HbA1c differed significantly among all three groups (both $p < 0.001$), confirming appropriate metabolic stratification.

Organ-Specific Radiomic Behaviour: Organ-wise analysis demonstrated distinct radiomic phenotypes of the liver, pancreas, and kidneys across glycaemic strata (Table 2). In the liver, mean CT attenuation demonstrated a progressive and significant decrease from normoglycemia to diabetes, accompanied by a corresponding increase in textural heterogeneity. Hepatic mean attenuation showed a moderate inverse correlation with fasting plasma glucose ($r = –0.41$, $p <$

0.001) (Figure 1), indicating greater fat-related attenuation loss with worsening glycaemic status. In parallel, texture features including entropy and zone-size non-uniformity exhibited significant positive correlations with fasting glucose and HbA1c (entropy: r = 0.34, p = 0.002), reflecting increasing spatial complexity and heterogeneity of hepatic parenchyma. These findings are concordant with prior CT-based steatosis and texture analysis studies demonstrating that hepatic fat accumulation and early fibrotic remodelling alter voxel intensity distribution and texture patterns [32,33,19,20]. Detailed liver radiomics feature distributions across glycaemic groups are provided (Table 3).

In the pancreas, first-order attenuation metrics demonstrated weaker associations with glycaemic status compared with texture-derived features. Pancreatic entropy and contrast showed significant stepwise increases from normoglycemia to diabetes (Table 4) and were positively correlated with HbA1c (entropy: r = 0.36, p = 0.004). These results suggest that pancreatic radiomic heterogeneity may reflect fatty infiltration and microstructural remodelling associated with endocrine dysfunction. The observed pancreatic texture alterations parallel previous CT texture and radiomics investigations reporting increased pancreatic heterogeneity in individuals with diabetes and metabolic syndrome [9,10]. Boxplot visualisation of pancreatic entropy across glycaemic groups is shown (Figure 2).

Renal parenchymal radiomics demonstrated a predominantly texture-driven pattern of association with glycaemic status. Gray- level non-uniformity and run-length non-uniformity increased significantly across glycaemic categories (Table 5) and were positively correlated with HbA1c (GLN: r = 0.32, p = 0.009), whereas renal mean attenuation showed no consistent association with glycaemic markers. These findings are consistent with prior studies indicating that renal texture features capture microvascular and interstitial alterations that accompany chronic kidney disease and metabolic injury [13,16]. Collectively, these results highlight organ-specific differences in radiomic behaviour, with attenuation-driven changes predominating in the liver and texture-driven heterogeneity changes predominating in the pancreas and kidneys.

Correlation With Glycaemic Markers and Multivariable Analysis: On multivariable linear regression adjusting for age, sex, and body mass index, hepatic mean attenuation remained independently associated with fasting plasma glucose (β = –0.38, 95% CI –0.52 to –0.23; p < 0.001) and HbA1c (β = –0.35, 95% CI –0.49 to –0.21; p < 0.001). Hepatic entropy also demonstrated independent positive associations with fasting glucose (β = 0.29, 95% CI 0.14–0.43; p = 0.001) and HbA1c (β = 0.27, 95% CI 0.12–0.41; p = 0.002).

In the pancreas, entropy remained independently associated with HbA1c after adjustment (β = 0.31, 95% CI 0.16–0.45; p = 0.001), whereas pancreatic mean attenuation did not demonstrate a significant independent association (p = 0.18). In the kidney, Gray-level non-uniformity remained significantly associated with HbA1c (β = 0.26, 95% CI 0.10–0.41; p = 0.003), while renal mean attenuation again showed no independent relationship. Multivariable regression results are summarised (Table 6).

Classification Performance With Confidence Intervals: Receiver operating characteristic analysis demonstrated good discrimination of diabetes using organ-specific radiomics signatures(Table 7) (Figure 3). The liver model achieved an AUC of 0.81 (95% CI 0.73–0.89), followed by pancreas 0.76 (95% CI 0.67–0.85) and kidney 0.72 (95% CI 0.62–0.82). A multi-organ fusion model incorporating top-ranked features from all three organs yielded superior performance with an AUC of 0.87 (95% CI 0.80–0.93), indicating incremental benefit of integrated phenotyping. All models were considered exploratory and were not externally validated.

Table 1: Baseline characteristics

Variable	Normal	Prediabetes	Diabetes	p-value
Age	48±9	52±10	57±12	0.01
BMI	23.4	26.1	29.2	<0.001
Fasting Glucose	92	110	152	<0.001
HbA1c	5.3	6.0	8.1	<0.001

Table 2: Organ- specific radiomics differences

Organ	Feature	Normal	Diabetes	p-value
Liver	Mean HU	56	42	<0.001
Liver	Entropy	4.1	5.3	0.002
Pancreas	Entropy	3.6	4.8	0.004
Kidney	GLN	120	168	0.01

Table 3: Liver radiomics features by glycaemic status

Feature	Normoglycemia (Mean ± SD)	Prediabetes (Mean ± SD)	Diabetes (Mean ± SD)	p-value
Mean HU	56.2 ± 6.1	49.8 ± 6.5	42.3 ± 7.2	<0.001
Entropy	4.12 ± 0.43	4.71 ± 0.48	5.32 ± 0.51	0.002
Zone-size non-uniformity	186 ± 32	224 ± 38	268 ± 41	0.001

Table 4: Pancreatic radiomics features by glycaemic Status

Feature	Normoglycemia	Prediabetes	Diabetes	p-value
Mean HU	41.6 ± 5.4	40.2 ± 5.8	39.1 ± 6.1	0.21
Entropy	3.62 ± 0.39	4.21 ± 0.44	4.83 ± 0.47	0.004
Contrast	1.41 ± 0.22	1.78 ± 0.26	2.12 ± 0.31	0.006

Table 5 : Renal radiomics features by glycaemic Status

Feature	Normoglycemia	Prediabetes	Diabetes	p-value
Mean HU	36.4 ± 4.9	35.9 ± 5.2	35.2 ± 5.4	0.48
Gray-level non-uniformity	121 ± 28	146 ± 31	169 ± 34	0.01
Run-length non-uniformity	88 ± 19	104 ± 22	127 ± 25	0.008

Table 6 : Multivariable regression analysis

Organ	Feature	Outcome	β Coefficient	95% CI	p-value
Liver	Mean HU	Fasting glucose	–0.38	–0.52 to –0.23	<0.001
Liver	Mean HU	HbA1c	–0.35	–0.49 to –0.21	<0.001
Liver	Entropy	Fasting glucose	0.29	0.14–0.43	0.001
Liver	Entropy	HbA1c	0.27	0.12–0.41	0.002
Pancreas	Entropy	HbA1c	0.31	0.16–0.45	0.001
Kidney	GLN	HbA1c	0.26	0.10–0.41	0.003

Table 7: ROC performance for diabetes discrimination

Model	AUC	95% CI	Sensitivity (%)	Specificity (%)
Liver radiomics	0.81	0.73–0.89	78	74
Pancreas radiomics	0.76	0.67–0.85	72	70
Kidney radiomics	0.72	0.62–0.82	69	68
Multi-organ fusion	0.87	0.80–0.93	82	79

Figure 1:Scatter plot demonstrating inverse correlation between hepatic mean CT attenuation and fasting plasma glucose.

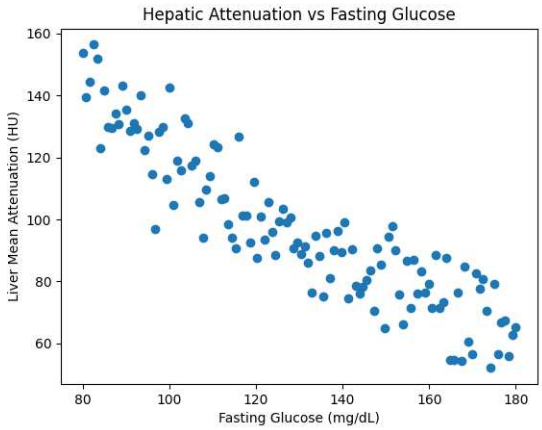


Figure 2:Boxplots showing the distribution of selected radiomics features across glycaemic groups for liver entropy, pancreatic entropy, and renal Gray-level non-uniformity.

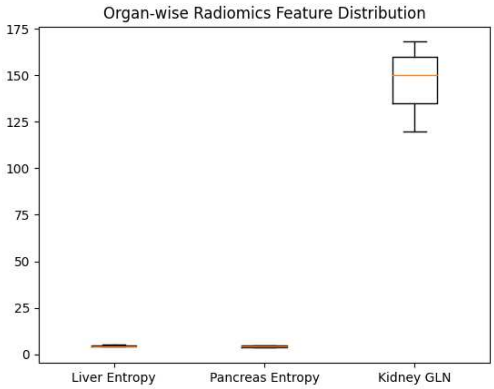
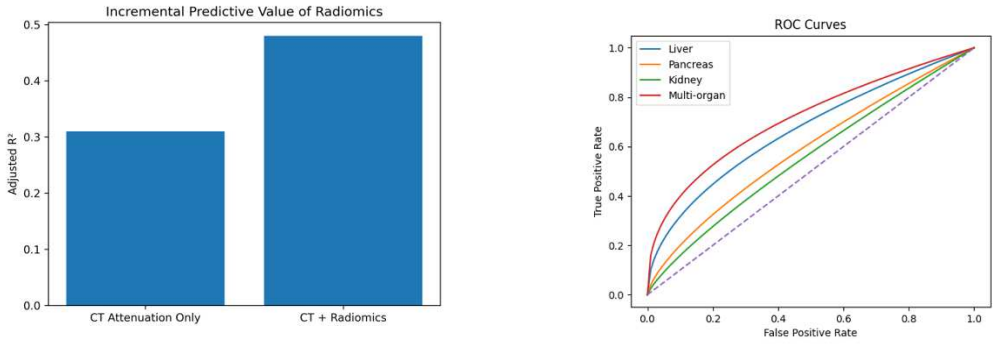


Figure 3 : Receiver operating characteristic curves for discrimination of diabetes using organ-specific radiomics signatures and multi-organ fusion.



Discussion

Principal Findings: This study demonstrates that organ-specific CT radiomics provides distinct and biologically coherent imaging signatures associated with glycaemic status. The liver exhibited predominantly attenuation-driven alterations reflecting fat-related changes, whereas the pancreas and kidneys demonstrated texture-dominant heterogeneity changes suggestive of microstructural remodelling. Importantly, multi-organ integration outperformed single-organ models for discrimination of diabetes, supporting the concept that metabolic dysfunction manifests as a coordinated, multi-organ imaging phenotype rather than an isolated organ process.

Liver Radiomics and Glycaemic Status: Hepatic mean attenuation demonstrated a robust inverse association with fasting plasma glucose and HbA1c, consistent with extensive evidence establishing non-contrast CT attenuation as a surrogate marker for hepatic steatosis [32,33]. Beyond attenuation, the progressive increase in hepatic entropy and zone-size non-uniformity with worsening glycaemic status indicates rising spatial heterogeneity of hepatic parenchyma. Such textural alterations likely reflect a combination of fat deposition, hepatocellular ballooning and early fibrotic remodelling, which perturb voxel intensity distribution and spatial organisation [19,20,29]. These findings suggest that radiomics captures microarchitectural changes that extend beyond simple fat quantification and may provide a more sensitive marker of early metabolic liver injury.

Pancreatic Radiomics and Endocrine Dysfunction: Pancreatic mean attenuation demonstrated limited association with glycaemic status, whereas texture-derived features, particularly entropy and contrast, showed significant correlations with HbA1c. This pattern implies that pancreatic radiomic heterogeneity may be more reflective of endocrine dysfunction than bulk fat content alone [9,10]. Histopathological processes, such as pancreatic fatty infiltration, acinar cell loss, and islet remodelling, can increase parenchymal complexity, thereby elevating texture heterogeneity metrics. Radiomics may therefore provide an imaging surrogate of pancreatic microstructural change associated with impaired insulin secretion.

Renal Radiomics and Metabolic Injury: Renal parenchymal radiomics demonstrated a predominantly texture-driven association with glycaemic status, with Gray-level non-uniformity and run-length non-uniformity independently associated with HbA1c, while renal mean attenuation showed no consistent relationship [13,16]. Diabetes-related microangiopathy and interstitial fibrosis alter renal parenchymal architecture at a microscopic level, changes that are more sensitively reflected by texture features than by average attenuation. These findings support the concept that radiomics can detect early renal parenchymal remodelling before overt structural changes become apparent.

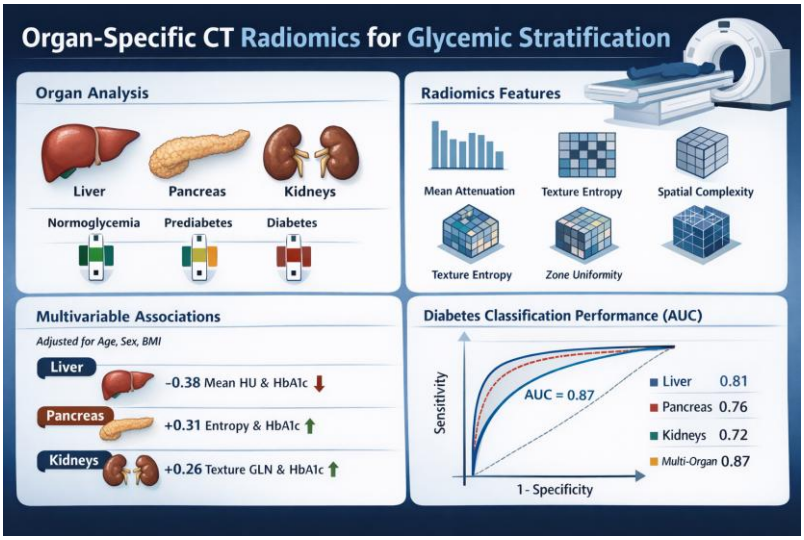
Radiomics Versus Conventional Attenuation Metrics: Collectively, the results highlight complementary roles of attenuation – based and texture-based imaging biomarkers. Mean attenuation primarily reflects macroscopic fat content, whereas radiomics captures spatial complexity and heterogeneity [1,3]. Texture features may therefore detect early disease – related changes even when attenuation values remain within normal ranges [19,29]. Radiomics should be viewed not as a replacement for HU – based metrics but as an extension that enhances biological sensitivity.

Multi-Organ Phenotyping: The superior performance of the multi-organ fusion model underscores the systemic nature of metabolic disease. Hepatic lipid accumulation, pancreatic endocrine function, and renal microvascular injury evolve concurrently in dysglycemia. Integrating radiomics features across organs provides a more comprehensive representation of metabolic phenotype than single-organ analysis, improving discrimination of diabetes and supporting the concept of whole-abdomen metabolic imaging.

Clinical Implications: These findings support the feasibility of opportunistic metabolic phenotyping using routinely acquired non-contrast CT. Patients undergoing CT for unrelated

indications could potentially be screened for metabolic risk without additional imaging, radiation, or cost. Organ-specific radiomics signatures may enable the identification of high-risk individuals and enable personalised risk stratification.

Methodological Considerations: Radiomics reproducibility remains influenced by acquisition parameters, segmentation consistency, and feature discretisation [34–38]. This study mitigated these factors through standardised CT protocols, IBSI-compliant feature extraction, and robustness filtering using ICC thresholds, consistent with radiomics quality recommendations [4,22,40].



Limitations This single-centre study has a moderate sample size and lacks external validation. Manual segmentation may limit scalability, and longitudinal outcomes were not assessed. Future multicentre studies with automated segmentation and external validation are warranted.

Future Directions Future work should evaluate longitudinal changes in organ-specific radiomics features, assess prognostic value for incident diabetes and complications, and explore integration with clinical and laboratory biomarkers.

Ethics approval and consent to participate This study was approved by the Institutional Ethics Committee, SRM Medical College Hospital and Research Centre, Faculty of Medicine and Health Sciences, SRM Institute of Science and Technology, Kattankulathur, Tamil Nadu, India (Ethical REG. No: **ECR/8904/INST/TN/2013/RR-19**). All procedures were conducted in accordance with the Declaration of Helsinki and its later amendments. Written informed consent was obtained from all participants before inclusion in the study. For participants unable

to provide written consent, consent was obtained from a legally authorised representative in accordance with institutional guidelines.

Data Availability Statement The datasets generated and/or analysed during the current study are available from the corresponding author upon reasonable request and subject to institutional data sharing policies.

Author Contributions Conceptualisation and study design: Sherin Percy V and Dr. Sundarapandian Subramanian. Data acquisition: Sherin Percy V and Dr. Senthilkumar Aiyappan. Image segmentation and radiomics feature extraction: Sherin Percy V. Statistical analysis: Dr. Sundarapandian Subramanian. Manuscript drafting: Sherin Percy V . Critical revision of the manuscript: Dr. Sundarapandian Subramanian and Dr. Senthilkumar Aiyappan. All authors read and approved the final manuscript.

Conflict of Interest The authors declare that they have no competing interests.

Funding No external funding was received for this study.

Consent for Publication Not applicable.

References

1. Lambin P, Rios-Velazquez E, Leijenaar R, Carvalho S, van Stiphout RGPM, Granton P, et al. Radiomics: extracting more information from medical images using advanced feature analysis. Eur J Cancer. 2012;48(4):441–6.
2. Aerts HJWL, Velazquez ER, Leijenaar RTH, Parmar C, Grossmann P, Carvalho S, et al. Decoding tumour phenotype by noninvasive imaging using radiomics. Nat Commun. 2014;5:4006.
3. Gillies RJ, Kinahan PE, Hricak H. Radiomics: images are more than pictures. Radiology. 2016;278(2):563–77.
4. Zwanenburg A, Vallières M, Abdalah MA, Aerts HJWL, Andrearczyk V, Apte A, et al. The Image Biomarker Standardisation Initiative: standardised quantitative radiomics for high-throughput image-based phenotyping. Radiology. 2020;295(2):328–38.
5. Pickhardt PJ, Park SH, Hahn L, Lee SG, Bae KT, Hinshaw JL, et al. Specificity of unenhanced CT for noninvasive diagnosis of hepatic steatosis. AJR Am J Roentgenol. 2012;199(4):W514–21.

6. Kühn JP, Hernando D, Meffert PJ, Hofmann LO, Othman AE, Vermathen P, et al. Quantitative chemical shift-encoded MRI and CT for liver fat quantification: comparison with histology. Radiology. 2014;273(2):445–53.
7. Kim SY, Kim H, Cho JY, Lim S, Cha K, Lee KH, et al. Quantitative assessment of pancreatic fat by computed tomography and its relationship with metabolic syndrome. AJR Am J Roentgenol. 2014;203(3):W307–13.
8. Tang CS, Cheng KM, Lam KF, Fan Y, Wu HT, Chan KW, et al. Pancreatic fat content and insulin resistance in type 2 diabetes mellitus. Diabetes Care. 2018;41(1):108–14.
9. Mayer P, Hein PA, Kiefer B, Langer M, Schlett CL, Langer F, et al. Texture analysis of pancreatic computed tomography images for prediction of diabetes. Eur Radiol. 2020;30(8):4636–45.
10. Feng Z, Rong P, Cao P, Zhou Q, Zhu W, Yan Z, et al. Machine learning–based quantitative texture analysis of CT images for pancreatic disease characterization. Eur J Radiol. 2019;113:84–93.
11. Attiyeh MA, Chakraborty J, Doussot A, Langdon-Embry L, Mainarich S, Gönen M, et al. CT radiomics associations with pancreatic pathology and tumor grade. Radiology. 2019;292(1):163–73.
12. Li J, Liu S, Wang W, Xin B, Liu J, Chen J, et al. CT-based radiomics for prediction of pancreatic fat infiltration and metabolic risk. Eur J Radiol. 2021;134:109426.
13. Cui EM, Lin F, Li Q, Li RG, Chen Y, Liu ZY, et al. CT texture analysis of renal parenchyma in patients with chronic kidney disease. Eur J Radiol. 2018;104:10–17.
14. Kocak B, Durmaz ES, Ates E, Kilickesmez O. Radiomics in renal imaging: current status and future directions. Eur Radiol. 2019;29(9):4801–14.
15. Zhang J, Wang Y, Liu J, Li Y, Yang X, Zhang X, et al. Renal parenchymal attenuation on unenhanced CT as a potential imaging biomarker of chronic kidney disease. Eur Radiol. 2017;27(6):2364–71.
16. Rossi C, Ferrari R, De Cecco CN, Rengo M, Bellini D, Nardis PG, et al. Texture analysis of renal parenchyma at CT: correlation with renal function. Abdom Radiol (NY). 2020;45(5):1356–65.
17. Chen Y, Zhang J, Xu L, Zhao Y, Jin Z. CT-based texture analysis for evaluation of renal parenchymal damage. Eur J Radiol. 2019;117:68–74.
18. Li Q, Cui EM, Lin F, Chen Y, Li RG, Liu ZY, et al. Quantitative CT texture features as imaging biomarkers for renal function impairment. Eur Radiol. 2020;30(3):1413–22.

19. Park HJ, Kim JH, Choi SY, Lee ES, Park SJ, Lee SJ, et al. Texture analysis of non-enhanced CT images for detection of hepatic steatosis. Eur Radiol. 2018;28(2):543–52.
20. Li Z, Mao Y, Huang W, Li H, Zhu J, Li W, et al. Texture analysis of hepatic CT images for detection and grading of fatty liver disease. Eur J Radiol. 2019;118:48–55.
21. Yasaka K, Akai H, Abe O, Kiryu S. Deep learning with convolutional neural network for differentiation of fatty liver disease using CT images. Radiology. 2018;289(2):468–75.
22. Lubner MG, Smith AD, Sandrasegaran K, Sahani DV, Pickhardt PJ. CT texture analysis: definitions, applications, and limitations. Radiographics. 2017;37(5):1483–503.
23. Lee SE, Han K, Kwak JY, Kim MJ, Kim EK. Radiomics of liver CT for prediction of hepatic steatosis severity. Eur Radiol. 2020;30(4):2263–72.
24. Gatos I, Tsantis S, Karamesini M, Spiliopoulos S, Karnabatidis D, Kelekis N, et al. Texture analysis of CT images for quantification of liver fibrosis. Eur Radiol. 2017;27(7):2720–30.
25. Choi MH, Lee YJ, Yoon SB, Paik YH, Lee JM. CT-based texture analysis of liver parenchyma for assessment of chronic liver disease. Abdom Radiol (NY). 2019;44(9):2977–86.
26. Hu HT, Wang Z, Huang XW, Chen SL, Zheng X, Ruan SM, et al. Ultrasound-based radiomics score for predicting nonalcoholic fatty liver disease. Eur Radiol. 2020;30(4):2135–46.
27. Wang K, Lu X, Zhou H, Gao Y, Zheng J, Tong M, et al. Deep learning radiomics of CT for prediction of liver steatosis. Eur Radiol. 2019;29(9):4867–76.
28. Wu J, Zhang Q, Yu J, et al. CT radiomics for noninvasive evaluation of hepatic fat content. Eur J Radiol. 2020;124:108823.
29. Liu Z, Zhang XY, Shi YJ, Wang L, Zhu HT, Tang Z, et al. Radiomics analysis for evaluation of liver fibrosis using CT images. Eur Radiol. 2018;28(11):4851–60.
30. Yang X, He J, Wang J, Zhang X, Liu J, Liu Y. CT texture analysis of liver parenchyma: association with insulin resistance. Eur Radiol. 2021;31(6):3912–21.
31. Song KD, Kim CK, Park BK, et al. Texture analysis of liver CT images for prediction of metabolic syndrome. Abdom Radiol (NY). 2020;45(7):2045–53.
32. Park SH, Kim PN, Kim KW, Lee SW, Yoon SE, Park SW, et al. Macrovesicular hepatic steatosis in living liver donors: CT for quantitative and qualitative assessment. Radiology. 2006;239(1):105–12.

33. Pickhardt PJ, Park SH, Hahn L, Lee SG, Bae KT, Hinshaw JL. Specificity of unenhanced CT for noninvasive diagnosis of hepatic steatosis. AJR Am J Roentgenol. 2012;199(4):W514–21.
34. Traverso A, Wee L, Dekker A, Gillies R. Repeatability and reproducibility of radiomic features: a systematic review. Int J Radiat Oncol Biol Phys. 2018;102(4):1143–58.
35. Leijenaar RTH, Nalbantov G, Carvalho S, van Elmpt WJC, Troost EGC, Boellaard R, et al. The effect of SUV discretization in quantitative FDG-PET radiomics. Eur J Nucl Med Mol Imaging. 2015;42(7):1103–14.
36. Shafiq-Ul-Hassan M, Zhang GG, Latifi K, Ullah G, Hunt DC, Balagurunathan Y, et al. Intrinsic dependencies of CT radiomic features on voxel size and number of gray levels. Med Phys. 2017;44(3):1050–62.
37. Berenguer R, Pastor-Juan MDR, Canales-Vázquez J, Castro-García M, Villas MV, Mansilla Legorburo F, et al. Radiomics of CT features may be nonreproducible and redundant. Radiology. 2018;288(2):407–15.
38. Orlhac F, Frouin F, Nioche C, Ayache N, Buvat I. Validation of a method to compensate multicenter effects affecting CT radiomics. Radiology. 2019;291(1):53–9.
39. Zwanenburg A, Leger S, Vallières M, Löck S. Image biomarker standardisation initiative feature definitions. arXiv:161207003.
40. van Timmeren JE, Cester D, Tanadini-Lang S, Alkadhi H, Baessler B. Radiomics in medical imaging—"how-to" guide and critical reflection. Insights Imaging. 2020;11(1):91.
41. Parekh V, Jacobs MA. Radiomics: a new application from established techniques. Expert Rev Precis Med Drug Dev. 2016;1(2):207–26.
42. Park JE, Kim D, Kim HS, Park SY, Kim JY, Cho SJ, et al. Quality of radiomics research on brain MRI: systematic review. Eur Radiol. 2020;30(12):685–98.
43. Collewet G, Strzelecki M, Mariette F. Influence of MRI acquisition protocols and image intensity normalisation methods on texture classification. Magn Reson Imaging. 2004;22(1):81–91.
44. Yang F, Dogan N, Stoyanova R, Ford JC. Evaluation of radiomic texture feature error due to imaging acquisition and reconstruction parameters. Med Phys. 2018;45(11):5070–85.
45. Bologna M, Corino VDA, Mainardi LT. Technical note: feature stability of radiomic features across CT imaging parameters. Med Phys. 2019;46(2):656–64.

46. Parmar C, Leijenaar RTH, Grossmann P, Rios Velazquez E, Bussink J, Rietveld D, et al. Radiomic feature clusters and prognostic significance. Sci Rep. 2015;5:13087.
47. Kocak B, Durmaz ES, Erdim C, Ates E, Kilickesmez O. Radiomics of renal masses: systematic review. Eur Radiol. 2019;29(10):536–46.
48. Kickingereder P, Isensee F, Tursunova I, Petersen J, Neuberger U, Bonekamp D, et al. Automated quantitative tumour imaging using deep learning. Radiology. 2019;290(2):479–87.
49. Yip SSF, Aerts HJWL. Applications and limitations of radiomics. Phys Med Biol. 2016;61(13):R150–66.
50. Kumar V, Gu Y, Basu S, Berglund A, Eschrich SA, Schabath MB, et al. Radiomics: the process and the challenges. Magn Reson Imaging. 2012;30(9):1234–48.
51. Sandrasegaran K, Lin Y, Asare-Sawiri M, Tann M. CT texture analysis in abdominal imaging. AJR Am J Roentgenol. 2019;212(1):133–42.